Development and Application of Rail Transit Capacity Models in Taiwan

Jyh-Cherng Jong, Yung-Cheng (Rex) Lai, Sheng-Hsuan Huang, and Pei-Chun (Sofi) Chiang

Rail transit systems are often the backbone of the transportation system in major cities; hence, the quality of the systems usually has a substantial impact on overall transportation efficiency. The assessment of the level of service and rail capacity plays an important role in monitoring the performance of an existing system and determining whether to undertake new resource planning projects. In this study the general concepts in the TCRP *Transit Capacity and Quality of Service Manual* were adopted, followed by the development of a set of comprehensive capacity models with consideration of modern signaling systems and a complete set of possible movements at critical track layouts. These models were implemented and validated by rail transit operators in Taiwan according to the operational data and practices. The proposed capacity models can help rail transit operators with similar operational environments to monitor their systems' performance and identify critical bottlenecks.

Rail transit systems are often the backbone of the transportation system in major cities (*1–3*); hence, the quality of the systems usually has a substantial impact on overall transportation efficiency. The assessment of the level of service and rail capacity plays an important role in monitoring the performance of an existing system and determining whether to undertake a new resource planning project. In general, rail capacity can be defined as a measure of the ability to move a specific amount of traffic over a defined rail line under a specific service plan (or level of service) in a given period of time, typically an hour for transit systems (*4, 5*).

Rail transit capacity is highly dependent on the type of signaling system and critical track layouts (*1*). Whereas the possible types of track layouts have remained almost unchanged for decades, signaling systems have evolved significantly over time (*6, 7*). For example, apart from three-aspect signaling systems, one of the Taipei Mass Rapid Transit (TMRT) lines recently adopted the latest moving-block system with communication-based train control, and the rest of the TMRT lines are all controlled by speed codes (*8–12*). In addition, the distance-to-go system used by Kaohsiung Mass Rapid Transit (KMRT) is also a popular signaling system adopted by many transit agencies (*12*). The development of suitable rail transit capacity models for these systems with new types of signaling systems is thus highly desirable.

The most popular tool for evaluation of rail transit capacity is in Part 5 of the TCRP *Transit Capacity and Quality of Service Manual* (TCQSM) (*1*). TCQSM, which is based on operating experiences from earlier decades in North America, presents a general approach to determining rail transit capacity. However, it has some deficiencies when applied to the TMRT and KMRT systems (*11, 12*). For instance, the discussion of the signal headway of turnbacks in TCQSM is limited to terminals with island platforms and forward scissors crossovers; however, terminals with side platforms should also be accounted for, and the location (forward or rear) of the crossovers should be considered. In addition, TCQSM assumes that the spacing between trains is at least double the safe stopping distance; this may be too conservative, especially for systems with modern signaling systems (*12*).

To provide the metro agencies in Taiwan a more robust capacity evaluation tool, this research adopted some of the general concepts in TCQSM and then developed more generic and comprehensive capacity models according to the operating practices of and data provided by TMRT and KMRT. The proposed capacity models can help rail transit operators with similar operational environments to monitor their systems' performance and identify critical bottlenecks.

RAIL TRANSIT CAPACITY

Rail capacity is defined here as maximum hourly throughput, which is predominantly affected by the types of signaling systems and the critical track layouts (*13*). The following sections briefly introduce several types of modern rail transit signaling systems and a set of critical track layouts, after which the development of the capacity models is described.

Modern Signaling Systems for Rail Transit

Modern rail transit signaling systems can be divided into systems with (*a*) speed codes, (*b*) distance to go, and (*c*) moving blocks (*1, 12, 14*). The differences in braking performance for these three systems (Figure 1) affect the headway between trains and the line capacity (*11*).

For a signaling system governed by speed codes, the continuous control systems enable information about the speed limits of a specific block to transmit along the track circuit (Figure 1*a*) (*15, 16*). Two types of speed codes are constantly transmitted to the train: (*a*) maximum safety speed (MSS) and (*b*) target speed (TS) (Figure 1*a*). The distance-to-go system eliminates one excessive empty block (Block A7) in the speed code system by transmitting the target stopping point

J.-C. Jong and S.-H. Huang, Civil and Hydraulic Engineering Research Center, Sinotech Engineering Consultants, Inc., No. 171, Nanking East Road, Sec. 5, Taipei, Taiwan, 10570. Y.-C. Lai and P.-C. Chiang, Department of Civil Engineering, National Taiwan University, Room 313, Civil Engineering Building, No. 1, Roosevelt Road, Sec. 4, Taipei, Taiwan, 10617. Corresponding author: Y.-C. Lai, yclai@ntu.edu.tw.

Transportation Research Record: Journal of the Transportation Research Board, No. 2216, Transportation Research Board of the National Academies, Washington, D.C., 2011, pp. 125–138.
DOI: 10.3141/2216-14

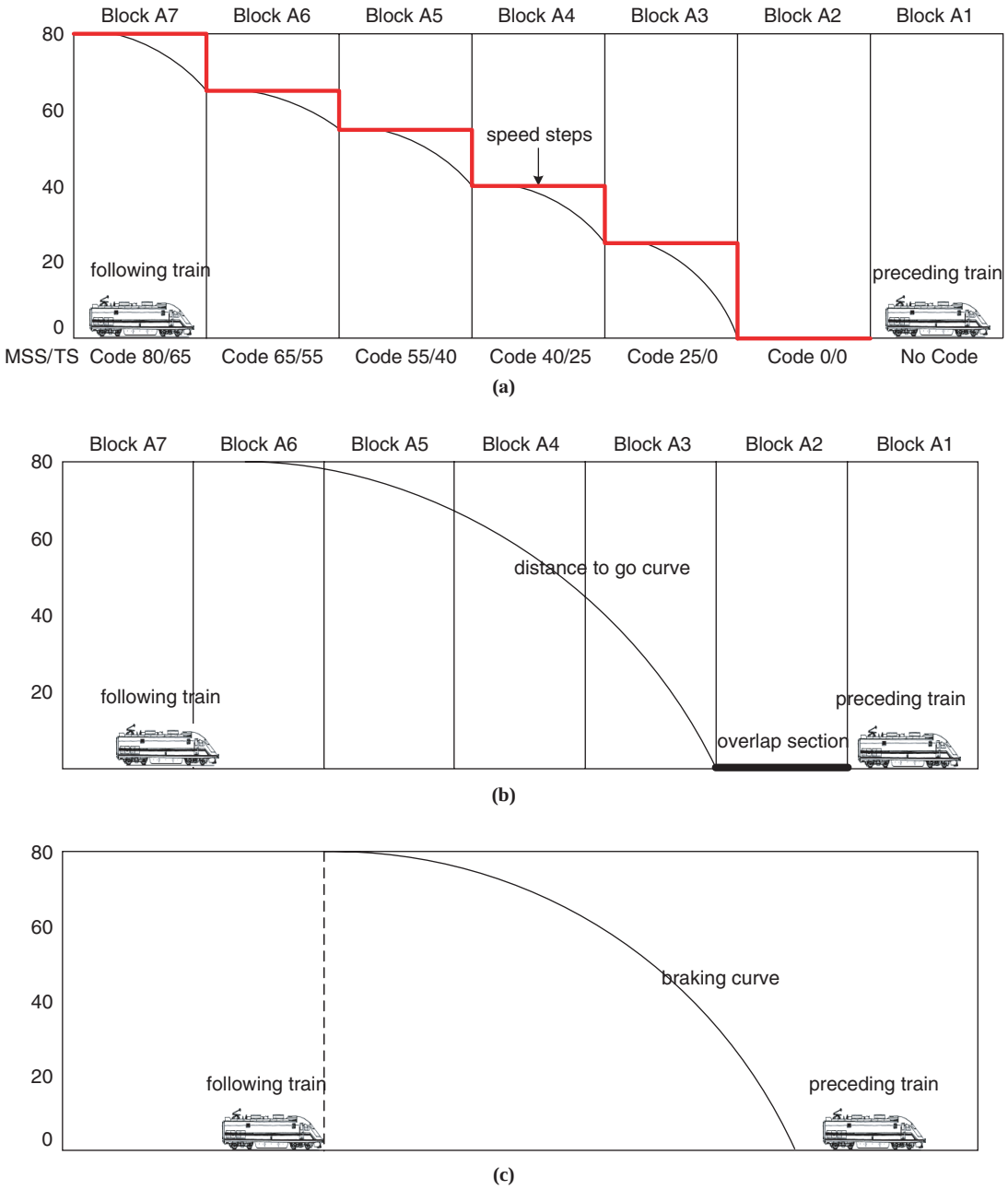

FIGURE 1 Train braking patterns of signaling systems with (*a*) speed codes, (*b*) distance to go, and (*c*) moving blocks.

to the onboard computer, generating the braking curve dynamically (Figure 1*b*) (*15*, *16*). For a moving-block system, the separation between trains is primarily based on the safe stopping distance (Figure 1*c*). Each train transmits its identity, location, and speed to an area computer that continuously makes the calculations for safe train separation and transmits this information to the following train (*16*–*20*).

Critical Track Layouts

In a transit system, the critical track layouts are those locations that may become capacity bottlenecks. According to TCQSM, intermediate stations, turnback locations, and junctions are usually the critical locations (*1*). Along with the locations of the crossover and possible turnback operations, seven possible types of movements (Figure 2) and 10 scenarios may be posited. Each scenario should have its particular signal headway equation. The ten possible scenarios are

Type I. Intermediate stations (Figure 2*a*) where

Type I-1. The departing train has not reached the attainable track speed as it exited the overlay block.

Type I-2. The departing train has reached the attainable track speed before it passed through the overlap section.

Type II. Turnbacks with forward scissors crossover where trains share the same track (Figure 2*b*).

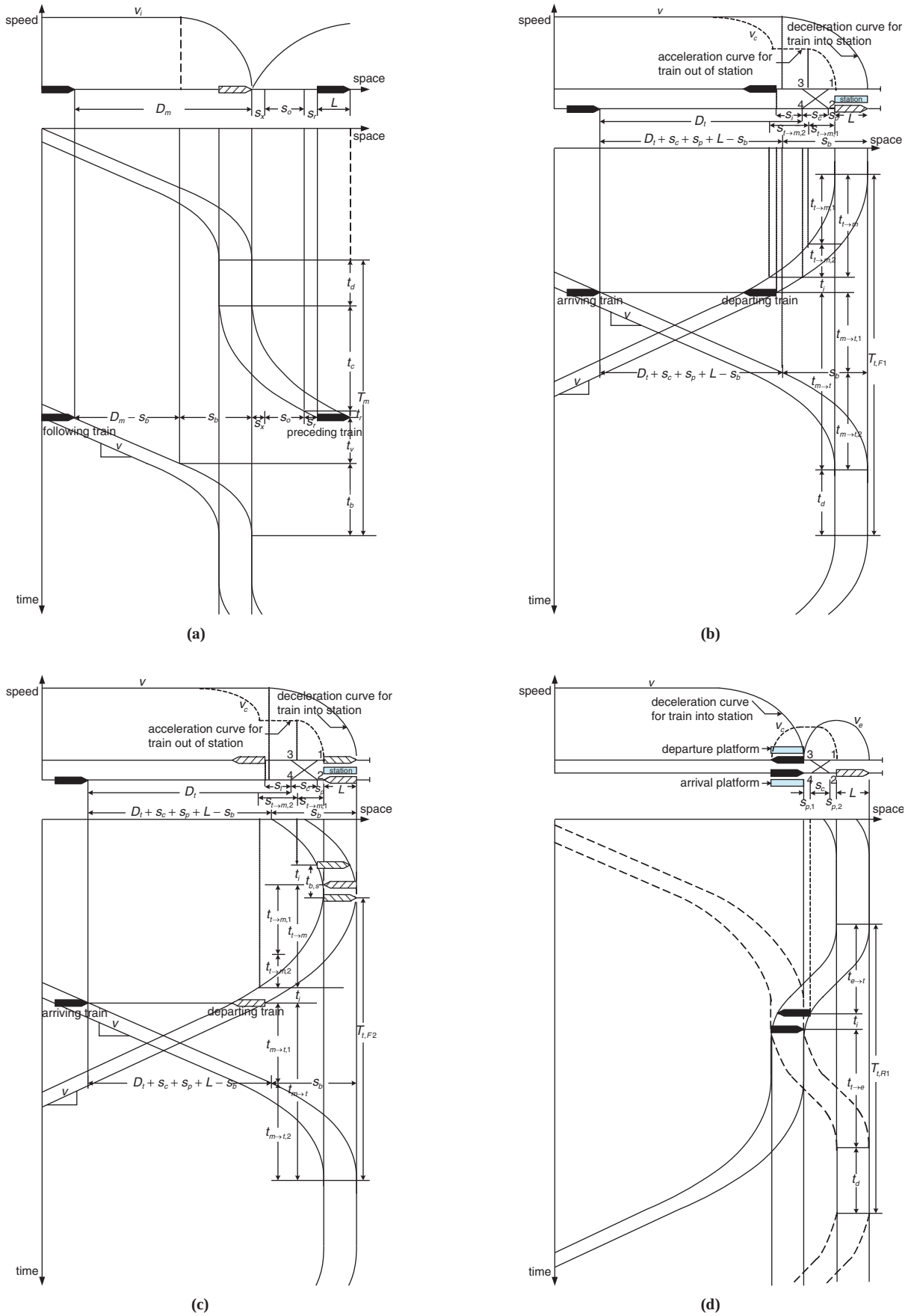

FIGURE 2 Signal headway of (*a*) Type I, (*b*) Type II, (*c*) Type III, (*d*) Type IV.

(continued on next page)

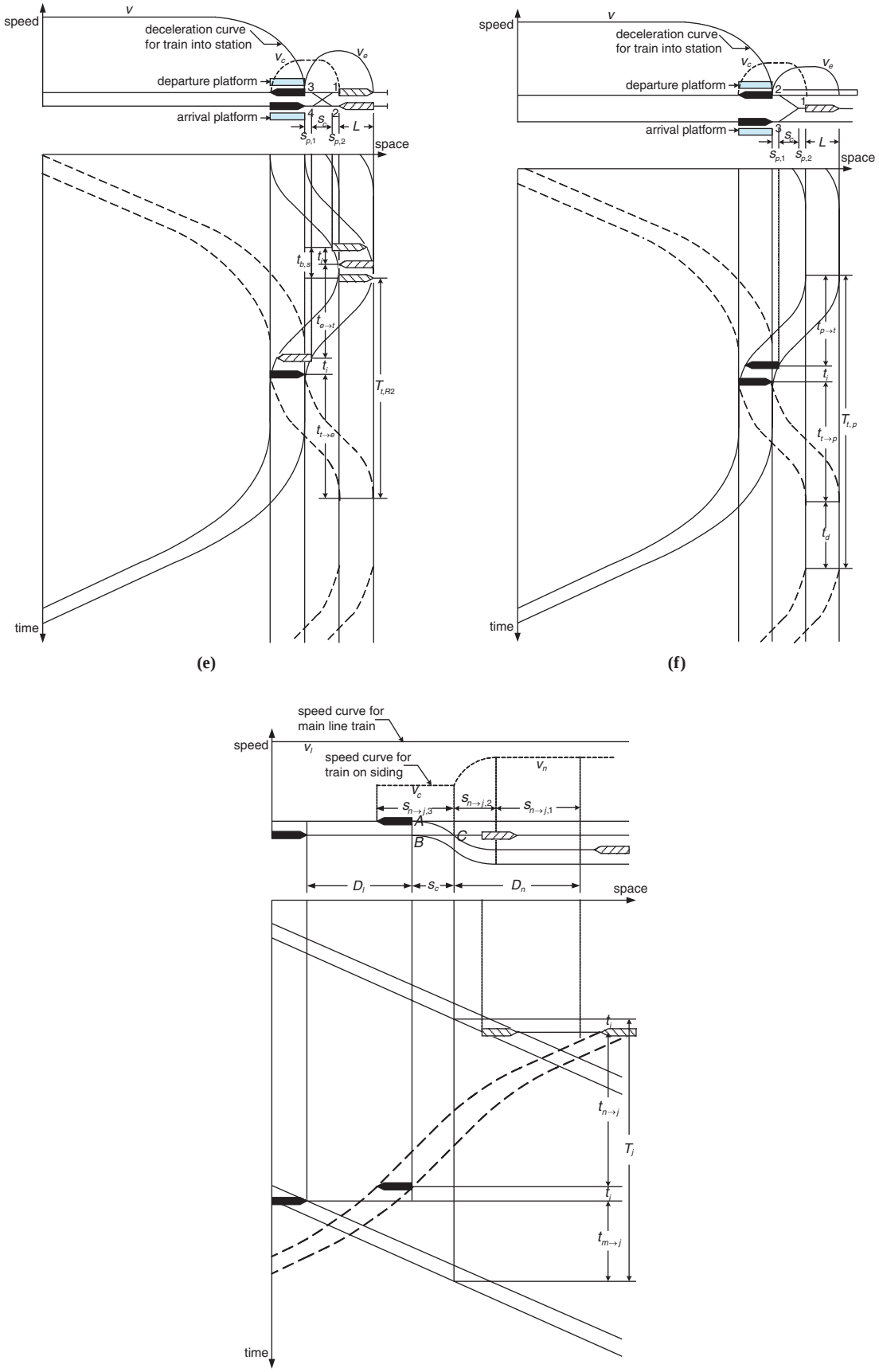

FIGURE 2 *(continued)* Signal headway of (*e*) Type V, (*f*) Type VI, and (*g*) Type VII movements at critical track layouts (see Table 1 for variable definitions).

Type III. Turnbacks with forward scissors crossover where trains use different tracks (Figure 2*c*) and

Type III-1. The track occupied by the first train has been cleared when the third train arrives.

Type III-2. The track occupied by the first train has not been cleared when the third train arrives.

Type IV. Turnbacks with rear scissors crossover where trains share the same track (Figure 2*d*).

Type V. Turnbacks with rear scissors crossover where trains use different tracks (Figure 2*e*) and

Type V-1. The track occupied by the first train has been cleared when the third train arrives.

Type V-2. The track occupied by the first train has not been cleared when the third train arrives.

Type VI. Turnbacks with pocket tracks (Figure 2*f*).

Type VII. Junctions (Figure 2*g*).

The current capacity models in TCQSM only cover the equations for Types I, III, and VII; this study aimed to develop a set of comprehensive capacity models covering all types of possible scenarios.

Computation Process of Rail Transit Capacity

The overall framework of rail transit capacity analysis for a given section is shown in Figure 3. The first phase of the framework is to estimate hourly train throughput (line capacity). Two principal factors determine line capacity: critical signal headway and operating margins. In the second phase, line capacity is converted into achievable capacity in number of passengers per hour based on the loading diversity and train capacity.

Critical Signal Headway

Signal headway is the minimal interval between successive trains passing a fixed point. The computation of signal headway in this study is based on blocking time, which is defined as the time interval during which a section of track is exclusively allocated to one train and therefore is blocked for other trains (*21*). The longer the blocking time, the longer the signal headway, and the lower the capacity. With the use of the notations in Table 1, Table 2 shows the 10 signal headway equations for the 10 possible scenarios described above. Three types of movements were chosen to demonstrate the derivation: (*a*) Type I-1 and I-2 scenarios to represent the movements at intermediate stations, (*b*) Type II scenario to show turnback operations, and (*c*) Type VII scenario to demonstrate the operations at junctions.

Signal Headway of Intermediate Stations (Types I-1 and I-2)

According to the TCRP project survey, intermediate stations should be the dominant limitation on throughput (*22*). Figure 2*a* and Equation 1 identify the components of signal headway for an intermediate station:

$$T_m = t_d + t_c + t_r + t_v + t_b \tag{1}$$

Station dwell time (t_d) is a model input. Each rail transit system should have its own operating practices on station dwell time; these can be different for different stations. For example, the station dwell time for major stations at TMRT is usually more than 40 s, while that for smaller stations is usually only 18 s.

The time for a train to clear the platform (t_c) can generally be formulated as

$$t_c = \sqrt{\frac{2(s_x + s_o + L)}{a}} \tag{2}$$

Equation 2 implies that the train is accelerating and will not reach its cruising speed (also called attainable track speed) as it exits the overlap section ($s_x + s_o + L \le v_o^2/2a$). If this train attains the line speed before passing through the overlap section ($s_x + s_o + L > v_o^2/2a$), then t_c is divided into two parts: $t_{c,1}$ (accelerating from rest to the cruising speed) and $t_{c,2}$ (operating at the cruising speed). Equation 5 can be derived as follows:

Let

$$s_a = \frac{v_o^2}{2a}$$

then

$$t_{c,1} = \frac{v_o}{a} \tag{3}$$

$$t_{c,2} = \frac{s_x + s_o + L - s_a}{v_o} = \frac{s_x + s_o + L}{v_o} - \frac{v_o}{2a} \tag{4}$$

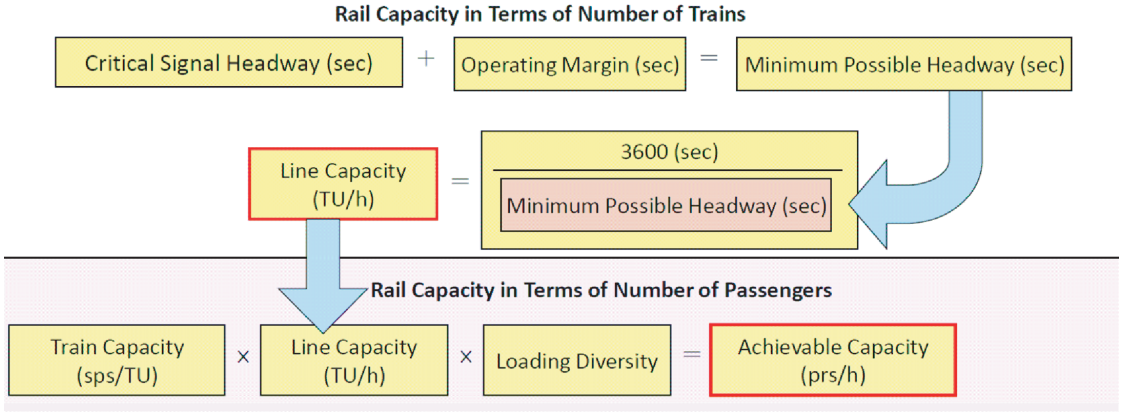

FIGURE 3 Capacity computation process (sps = spaces; prs = passengers).

TABLE 1 Notations in Rail Transit Capacity Models

Parameter	Description
A_v	Net floor area for standees (m^2/TU)
a	Service acceleration rate (m/s^2)
$a(G)$	Acceleration rate on grade G (m/s^2)
b	Service deceleration rate (m/s^2)
$b(G)$	Deceleration rate on grade G (m/s^2)
C_l	Line capacity (TU/h)
C_o	Design capacity (sps/h)
C_u	Achievable capacity (prs/h)
c_t	Train capacity (sps/TU)
D_m	Distance between the stopping location and the nearest position where the following train is allowed to approach (m)
D_t	Distance between the crossover and the nearest position where the following train is allowed to approach (m)
D_n	Distance between the crosspoint and the nearest position where the sideline train is allowed to approach (m)
D_l	Distance between the crosspoint and the nearest position where the mainline train is allowed to approach (m)
G_f	Grade at the forward scissors crossover of a turnback station (‰)
G_i	Grade before entering an intermediate station (‰)
$G_{j,l}$	Grade from mainline to a junction (‰)
$G_{j,n}$	Grade from sideline to a junction (‰)
G_o	Grade after exiting an intermediate station (‰)
G_p	Grade before entering the pocket track (‰)
G_r	Grade at the rear scissors crossover of a turnback station (‰)
h	Operating headway(s)
K_b	Braking safety factor
L	Train length (m)
m_s	Loading factor (prs/m^2)
n_s	Number of seats in a vehicle
Q_l	Separation safety factor for a mainline train at a junction
Q_m	Separation safety factor for trains at intermediate stations
Q_n	Separation safety factor for a sideline train at a junction
Q_t	Separation safety factor for a train entering the forward scissors crossover at a terminal station
r	The proportion of the bunching mainline trains to the total number of trains
s_a	Distance for a train to accelerate from stop to the cruising speed (m)
s_b	Braking distance (m)
s_c	Length of crossover (m)
s_o	Length of overlap block (m)
s_p	Distance from the forward crossover to where the train stops at the station (m)
$s_{p,1}$	Distance from where the train stops at the station to the rear crossover (m)
$s_{p,2}$	Distance from the crossover to where the train stops at the end of the track or at the pocket track (m)
s_{sb}	Safe braking distance (m)
s_x	Distance from where the train stops at the station block to the exit point of the block (m)
s_r	Reaction distance for driver and braking system (m)
$s_{t\to m,1}$	Distance for a train to accelerate from stop to the turnout speed within $s_{t\to m}$ (m)
$s_{t\to m,2}$	Distance for a train to travel at the turnout speed within $s_{t\to m}$ (m)
$s_{n\to j,1}$	Distance for a sideline train to travel at the cruising speed within $s_{n\to j}$ (m)
$s_{n\to j,2}$	Distance for sideline train to decelerate to turnout speed within $s_{n\to j}$ (m)
$s_{n\to j,3}$	Distance for a sideline train to travel at the turnout speed within $s_{n\to j}$ (m)
T_j	Signal headway of junctions (s)
T_m	Signal headway of an intermediate station (s)
T_t	Signal headway of a turnback station (s)
T_s	Critical signal headway (s)
$T_{t,F1}$	Signal headway of turnbacks with forward scissors crossover where trains share the same track (s)
$T_{t,F2}$	Signal headway of turnbacks with forward scissors crossover where trains use different tracks (s)
$T_{t,P}$	Signal headway of turnbacks where trains use pocket tracks (s)
$T_{t,R1}$	Signal headway of turnbacks with rear scissors crossover where trains share the same track (s)
$T_{t,R2}$	Signal headway of turnbacks with rear scissors crossover where trains use different tracks (s)
t_b	Time for a train to decelerate to full stop (s)
$t_{b,s}$	Time for a train to travel from the crossover to stop (s)
t_c	Time for a train to accelerate and exit a platform (s)
$t_{c,1}$	Time for a train to accelerate from stop to the cruising speed within t_c (s)
$t_{c,2}$	Time for a train to travel at the cruising speed within t_c (s)
t_d	Dwell time (s)
t_i	Switch throw and lock time (s)
t_m	Operating margins (s)
t_r	Reaction time for driver and control system (s)
t_v	Time for a train to proceed at cruising speed (s)
$t_{t\to m}$	Time for a departing train to traverse the crossover (s)
$t_{t\to m,1}$	Time for a train to acceleration to the turnout speed within $t_{t\to m}$ (s)
$t_{t\to m,2}$	Time for a train to travel at the turnout speed within $t_{t\to m}$ (s)
$t_{m\to t}$	Time for an arriving train to travel from the allowable nearest position to the station (s)
$t_{m\to t,1}$	Time for an arriving train to approach a terminal station at the cruising speed within $t_{m\to t}$ (s)
$t_{m\to t,2}$	Time for an arriving train to decelerate from cruising speed to stop within $t_{m\to t}$ (s)
$t_{n\to j}$	Time for a sideline train to travel from the allowable nearest point of the junction to pass the junction (s)
$t_{n\to j,1}$	Time for a sideline train to travel at cruising speed within $t_{n\to j}$ (s)
$t_{n\to j,2}$	Time for a sideline train to decelerate to the turnout speed within $t_{n\to j}$ (s)
$t_{n\to j,3}$	Time for a sideline train to travel at the turnout speed within $t_{n\to j}$ (s)
$t_{m\to j}$	Time for a mainline train to travel from the allowable nearest point of the junction to pass the junction (s)
$t_{e\to t}$	Time for a train to travel from the end of track and traverse the rear scissors crossover to stop at the station (s)
$t_{t\to e}$	Time for a train to travel from the platform and traverse the crossover to the end of the track (s)
$t_{t\to p}$	Time for a train to travel from the platform to enter the pocket track (s)
$t_{p\to t}$	Time for a train to travel from the pocket track to the platform (s)
v	Cruising speed between stations (m/s)
v_c	Turnout speed (m/s)
v_o	Cruising speed for a train leaving a station (m/s)
v_i	Cruising speed for a train entering a station (m/s)
v_l	Cruising speed for a mainline train approaching a junction (m/s)
v_n	Cruising speed for a sideline train approaching a junction (m/s)
v_e	Operating speed for a train entering the end of track after the rear scissors crossover (m/s)
β	Ratio of operating margins to critical signal headway
ρ_d	Loading diversity factor

TABLE 2 Equations of Signal Headways for Possible Scenarios

Scenario	Additional Condition	Equation for Computing Signal Headway
Type I-1	$s_x + s_o + L > \frac{v_o^2}{2a}$	$T_m = \frac{s_x + s_o + L}{v_o} + \frac{v_o}{2a(G_o)} + \frac{v_i}{2b(G_i)}\left(\frac{Q_m}{K_b} - 1\right) + \frac{v_i}{b(G_i)} + t_d + t_r$
Type I-2	$s_x + s_o + L \le \frac{v_o^2}{2a}$	$T_m = \sqrt{\frac{(s_x + s_o + L)}{a(G_o)}} + \frac{v_i}{2b(G_i)}\left(\frac{Q_m}{K_b} - 1\right) + \frac{v_i}{b(G_i)} + t_d + t_r$
Type II		$T_{t,F1} = \frac{s_c + s_p + L}{v_c} + \frac{v_c}{2a(-G_f)} + \frac{v}{2b(G_f)}\left(\frac{Q_t}{K_b} - 1\right) + \frac{s_c + s_p + L}{v} + \frac{v}{b(G_f)} + t_i + t_d$
Type III-1	$T_{t,F1} \ge 2(t_d + t_{b,s} - t_i)$	$T_{t,F2} = \frac{s_c + s_p + L}{v_c} + \frac{v_c}{2a(-G_f)} + \frac{v}{2b(G_f)}\left(\frac{Q_t}{K_b} - 1\right) + \frac{s_c + s_p + L}{v} + \frac{v}{b(G_f)} + 2t_i - \sqrt{\frac{2s_p}{b(G_f)}}$
Type III-2	$T_{t,F1} < 2(t_d + t_{b,s} - t_i)$	$T_{t,F2} = \frac{s_c + s_p + L}{2v_c} + \frac{v_c}{4a(-G_f)} + \frac{v}{4b(G_f)}\left(\frac{Q_t}{K_b} - 1\right) + \frac{s_c + s_p + L}{2v} + \frac{v}{2b(G_f)} + \frac{t_i + t_d}{2}$
Type IV		$T_{t,R1} = \frac{s_{p,1} + s_c + s_{p,2} + L}{v_c} + \frac{v_c}{2a(-G_r)} + \frac{v_c}{2b(-G_r)} - \sqrt{\frac{2s_{p,1}}{b(-G_r)}} + \sqrt{\frac{2b(G_r)(s_{p,1} + s_c + s_{p,2} + L)}{a(G_r)(a(G_r) + b(G_r))}} + \sqrt{\frac{2a(G_r)(s_{p,1} + s_c + s_{p,2} + L)}{b(G_r)(a(G_r) + b(G_r))}} + t_i + t_d$
Type V-1	$T_{t,R1} < 2(t_d + t_{b,s} - t_i)$	$T_{t,R2} = \frac{s_{p,1} + s_c + s_{p,2} + L}{v_c} + \frac{v_c}{2a(-G_r)} + \frac{v_c}{2b(-G_r)} - \sqrt{\frac{2s_{p,1}}{b(-G_r)}} + \sqrt{\frac{2b(G_r)(s_{p,1} + s_c + s_{p,2} + L)}{a(G_r)(a(G_r) + b(G_r))}} + \sqrt{\frac{2a(G_r)(s_{p,1} + s_c + s_{p,2} + L)}{b(G_r)(a(G_r) + b(G_r))}} + 2t_i - \sqrt{\frac{2s_{p,2}}{b(G_r)}}$
Type V-2	$T_{t,R1} < 2(t_d + t_{b,s} - t_i)$	$T_{t,R2} = \frac{s_{p,1} + s_c + s_{p,2} + L}{2v_c} + \frac{v_c}{4a(-G_r)} + \frac{v_c}{4b(-G_r)} - \sqrt{\frac{s_{p,1}}{2b(-G_r)}} + \sqrt{\frac{b(G_r)(s_{p,1} + s_c + s_{p,2} + L)}{2a(G_r)(a(G_r) + b(G_r))}} + \sqrt{\frac{a(G_r)(s_{p,1} + s_c + s_{p,2} + L)}{2b(G_r)(a(G_r) + b(G_r))}} + \frac{t_i + t_d}{2}$
Type VI		$T_{t,R2} = \frac{2(s_{p,1} + s_c + s_{p,2} + L)}{v_c} + \frac{v_c}{2a(-G_p)} + \frac{v_c}{2b(-G_p)} + \frac{v_c}{2a(G_p)} + \frac{v_c}{2b(G_p)} - \sqrt{\frac{s_{p,1}}{2b(-G_r)}} - \sqrt{\frac{s_{p,2}}{2b(-G_r)}} + t_i + t_d$
Type VII		$T_j = \frac{Q_l v_l}{2K_b b(G_{j,l})} + \frac{s_c + L}{v_l} + (1 - r)\frac{(Q_n - K_b)v_n}{2K_b b(G_{j,n})} + \frac{v_c^2}{2b(G_{j,n})v_n} + \frac{v_n - v_c}{b(G_{j,n})} + \frac{L + s_c}{v_c} + 2t_i$

$$t_c = t_{c,1} + t_{c,2} = \frac{v_o}{a} + \frac{s_x + s_o + L}{v_o} - \frac{v_o}{2a} = \frac{s_x + s_o + L}{v_o} + \frac{v_o}{2a} \tag{5}$$

Five seconds is recommended by TCQSM (*1*) for systems with automatic train operation.

Before deriving equations for t_v and t_b, several key elements related to braking and signaling should be discussed. To compute safe braking distance (s_{sb}), a constant, K_b, is added to address less-than-full braking efficiency, typically 75% of normal braking (*22*):

$$s_{sb} = \frac{v_i^2}{2K_b b} \tag{6}$$

Because of the uncertainty in detecting a train's location, it is difficult to precisely estimate the nearest position from which the following train is allowed to approach; therefore, D_m, the distance between the stopping location and the nearest position from which the following train is allowed to approach (Figure 2*a*), is estimated by using the safe braking distance times the separation safety factor (Q_m):

$$D_m = Q_m s_{sb} = \frac{Q_m v_i^2}{2K_b b} \qquad Q_m \ge 1 \tag{7}$$

According to operational data obtained from TMRT and KMRT, the recommended setting for Q_m is around (*a*) 1.5 to 2.0 for a speed

code system, (*b*) 1.0 to 1.2 for a distance-to-go system, and (*c*) 1.0 for a moving-block system.

The required time corresponding to s_b is t_b, and t_v represents the interval during which a train proceeds with line cruising speed.

$$t_b = \frac{v_i}{b} \tag{8}$$

$$t_v = \frac{D_m - s_b}{v_i} = \frac{Q_m s_{sb} - \frac{v_i^2}{2b}}{v_i} = \frac{v_i}{2b}\left(\frac{Q_m}{K_b} - 1\right) \tag{9}$$

The signal headway equations can now be rewritten as the following:

If

$$\frac{s_x + s_o + L \le v_o^2}{2a}$$

then

$$T_m = \sqrt{\frac{2(s_x + s_o + L)}{a}} + \frac{v_i}{2b}\left(\frac{Q_m}{K_b} - 1\right) + \frac{v_i}{b} + t_d + t_r \tag{10}$$

If

$$\frac{s_x + s_o + L > v_o^2}{2a}$$

then

$$T_m = \frac{s_x + s_o + L}{v_o} + \frac{v_o}{2a} + \frac{v_i}{2b}\left(\frac{Q_m}{K_b} - 1\right) + \frac{v_i}{b} + t_d + t_r \tag{11}$$

Signal Headway of Turnbacks (Type II)

To demonstrate how to develop the signal headway equations for turnbacks, Type II is used as an example.

Terminals with an island platform can serve two tracks passing on either side. Figure 2*b* and Equation 12 identify the components of signal headway for this scenario:

$$T_{t,F1} = t_{t\to m} + t_i + t_{m\to t} + t_d \tag{12}$$

Figure 2*b* illustrates this operation in three steps: (*a*) the train departing from the terminal (lower right) accelerates from rest, traverses the crossover, and then clears the crossover (Route 2→3) ($t_{t\to m}$); (*b*) the interlocking switch and signals are reset (t_i); and (*c*) the arriving train traverses the crossover ($t_{m\to t}$) and is fully berthed in the station (t_d).

Because of the difference in train speed, $t_{t\to m}$ can be divided into two parts:

$$t_{t\to m} = t_{t\to m,1} + t_{t\to m,2} \tag{13}$$

During $t_{t\to m,1}$, the train will accelerate from rest to the turnout speed (Equation 14); $s_{t\to m,1}$ is the distance corresponding to $t_{t\to m,1}$ (Equation 15):

$$t_{t\to m,1} = \frac{v_c}{a} \tag{14}$$

$$s_{t\to m,1} = \frac{v_c^2}{2a} \tag{15}$$

After $t_{t\to m,1}$, the train will traverse the crossover under the turnout speed until the end of this train clears the crossover. The duration of this movement is $t_{t\to m,2}$, which can be derived from $s_{t\to m,2}$:

$$s_{t\to m,2} = L + s_p + s_c - s_{t\to m,1} \tag{16}$$

$$t_{t\to m,2} = \frac{s_{t\to m,2}}{v_c} = \frac{L + s_p + s_c - s_{t\to m,1}}{v_c} = \frac{L + s_p + s_c}{v_c} - \frac{v_c}{2a} \tag{17}$$

Equation 13 can now be formulated as

$$t_{t\to m} = \frac{v_c}{a} + \frac{L + s_p + s_c}{v_c} - \frac{v_c}{2a} = \frac{L + s_p + s_c}{v_c} + \frac{v_c}{2a} \tag{18}$$

Similar to D_m, D_t is also estimated by using the separation safety factor (Q_t); the recommended values for Q_m can also be used for Q_t:

$$D_t = Q_t s_{sb} = \frac{Q_t v^2}{2K_b b} \qquad Q_t \ge 1 \tag{19}$$

After the interlocking switch and signals are reset (turnout is set to Route 4→2 in Figure 2*b*), the arriving train will be authorized to traverse the crossover and stop at the terminal. This period can be expressed by

$$t_{m\to t} = \frac{v}{2b}\left(\frac{Q_t}{K_b} - 1\right) + \frac{s_c + s_p + L}{v} + \frac{v}{b} \tag{20}$$

With Equations 18 and 20, Equation 12 can now be represented as

$$T_{1,F1} = \frac{L + s_p + s_c}{v_c} + \frac{v_c}{2a} + \frac{v}{2b}\left(\frac{Q_t}{K_b} - 1\right) + \frac{s_c + s_p + L}{v} + \frac{v}{b} + t_i + t_d \tag{21}$$

Signal Headway of Junctions (Type VII)

A level junction has a track configuration in which merging lines provide track connections with each other and thus require trains to cross over in front of opposing traffic at grade. A typical junction layout is illustrated in Figure 2*g*. The capacity of a level junction is determined in a similar manner to a turnback station.

Figure 2*g* illustrates this operation in two steps. First, the sideline train passes through the crosspoint (point C) right after the mainline train passes the same point ($t_{n\to j}$), and the turnout and signals are reset to the appropriate position (t_i). Next, after the first step and another t_i, the next mainline train passes through the crosspoint ($t_{m\to j}$).

The signal headway for junctions can be calculated as follows:

$$T_j = t_{n\to j} + t_{m\to j} + 2t_i \tag{22}$$

Similar to D_m, D_n is also estimated by using the separation safety factor (Q_n); the recommended values for Q_m can also be used for Q_n:

$$D_n = \frac{Q_n v_n^2}{2K_b b} \qquad Q_n \ge 1 \tag{23}$$

Because of the trailing-point movement, the sideline train must reduce its speed before it passes through the crosspoint. As a result of this speed difference, $t_{n\to j}$ can be divided into three parts: (*a*) operating at cruising speed ($t_{n\to j,1}$), (*b*) operating from cruising speed to turnout speed ($t_{n\to j,2}$), and (*c*) operating at turnout speed ($t_{n\to j,3}$):

$$t_{n\to j} = t_{n\to j,1} + t_{n\to j,2} + t_{n\to j,3} \tag{24}$$

The transitional speed ($t_{n\to j,2}$) and the distance corresponding to $t_{n\to j,2}$ can be calculated as follows:

$$t_{n\to j,2} = \frac{v_n - v_c}{b} \tag{25}$$

$$s_{n\to j,2} = \frac{v_n^2 - v_c^2}{2b} \tag{26}$$

The time and distance for the sideline train traveling at cruising speed would be

$$s_{n\to j,1} = D_n - s_{n\to j,2} = \frac{Q_n v_n^2}{2K_b b} - \frac{v_n^2 - v_c^2}{2b} = \frac{(Q_n - K_b)v_n^2}{2K_b b} + \frac{v_c^2}{2b} \tag{27}$$

$$t_{n\to j,1} = \frac{(Q_n - K_b)v_n}{2K_b b} + \frac{v_c^2}{2bv_n} \tag{28}$$

The third part refers to the situation in which the sideline train travels at the turnout speed until the end of the train passes through the crosspoint. Both the time and distance of this part of the movement can be formulated as

$$s_{n\to j,3} = L + s_c \tag{29}$$

$$t_{n\to j,3} = \frac{L + s_c}{v_c} \tag{30}$$

According to Equations 25, 28, and 30, Equation 24 can now be rewritten as

$$t_{n\to j} = \frac{(Q_n - K_b)v_n}{2K_b b} + \frac{v_c^2}{2bv_n} + \frac{v_n - v_c}{b} + \frac{L + s_c}{v_c} \tag{31}$$

D_l is required to compute $t_{m\to j}$; this value can be estimated by using the separation safety factor (Q_l). Again, the recommended values for Q_n can be used for Q_l:

$$D_l = \frac{Q_l v_l^2}{2K_b b} \qquad Q_l \geq 1 \tag{32}$$

With the facing-point movement, instead of reducing speed, the mainline train travels at its cruising speed as it passes through the crosspoint; therefore, $t_{m\to j}$ can be formulated as

$$t_{m\to j} = \frac{D_l + s_c + L}{v_l} = \frac{Q_l v_l}{2K_b b} + \frac{s_c + L}{v_l} \tag{33}$$

Equation 22 can now be reformulated by using Equations 31 and 33:

$$T_j = \frac{(Q_n - K_b)v_n}{2K_b b} + \frac{v_c^2}{2bv_n} + \frac{v_n - v_c}{b} + \frac{L + s_c}{v_c} + \frac{Q_l v_l}{2K_b b} + \frac{s_c + L}{v_l} + 2t_l \tag{34}$$

Equation 34 was derived with the assumption that one mainline train and one sideline train will pass through the crosspoint alternately. However, in normal practice, a sideline train often waits for several mainline trains to pass by before it can pass the junction. Therefore, in this study *r* was used to adjust this headway (*r* is defined as the proportion of the bunching mainline trains to the total number of trains, including sideline trains). T_j would be modified as

$$\begin{aligned} T_j &= rt_{m\to j} + (1-r)(t_{n\to j} + t_{m\to j} + 2t_i) = t_{m\to j} + (1-r)(t_{n\to j} + 2t_i) \\ &= \frac{Q_l v_l}{2K_b b} + \frac{s_c + L}{v_l} + (1-r)\left(\begin{array}{l} \dfrac{(Q_n - K_b)v_n}{2K_b b} + \dfrac{v_c^2}{2bv_n} \\ + \dfrac{v_n - v_c}{b} + \dfrac{L + s_c}{v_c} + 2t_i \end{array} \right) \end{aligned} \tag{35}$$

Signal headway varies with the types of movements at critical track layouts and operating patterns. There is no general formula to calculate signal headway for all kinds of possible bottlenecks on a transit line. However, by using Equation 36 the most critical bottleneck of a line can be selected:

$$T_s = \max(T_m, T_t, T_j) \tag{36}$$

Operating Margin

The operating margin is defined as the amount of time a train could be behind schedule without interfering with the trains following it (*1*). In this study, it was found that operating margins are dependent on the characteristics of a rail transit system. Instead of adopting a constant value, it is recommended that the operating margin be proportional to the critical signal headway so that it can reflect the relationship with the characteristics of rail systems and accommodate random effects (*23*, *24*). Equation 37 is the formulation for computing operating margin (t_m); β is the ratio of operating margin to critical signal headway:

$$t_m = \beta T_s \tag{37}$$

Average Headway

For any two successive trains, the minimum possible headway is calculated by the summation of critical signal headway and operating margins. On average, trains are allowed to run through a section every *h* seconds, which can be obtained by Equation 38:

$$h = T_s + t_m = (1+\beta)T_s \tag{38}$$

Hourly Train Throughput

The maximum service frequency (C_l) that can be achieved would be the line capacity:

$$C_l = \frac{3600}{h} = \frac{3600}{(1+\beta)T_s} \tag{39}$$

After obtaining C_l, the achievable capacity in number of passengers per hour can be computed according to the train capacity and design capacity.

Train Capacity

Train capacity (c_t) is dependent on the number of seats (n_s) and the size of the standing area (A_v) (Equation 40). The loading factor (m_s) should be used as an index to describe the riding comfort.

$$c_t = n_s + (m_s \times A_v) \tag{40}$$

Design Capacity

From the supply-side point of view, the maximum capability to transport passengers or the maximum offered capacity is defined as design capacity (C_o), which can be calculated by

$$C_o = C_l \times c_t \tag{41}$$

Achievable Capacity

In reality, passengers do not load evenly into cars and trains at all times (*1, 22, 25*). The loading diversity factor (ρ_d) is used to describe this fluctuation. Achievable capacity in Equation 42 represents the maximum number of passengers that can be transported:

$$C_u = \rho_d C_o \tag{42}$$

CASE STUDY

In this case study, three rail transit lines in Taiwan with three modern signaling systems were chosen to demonstrate and validate the proposed capacity models. They are the Blue Line (Yongning–Nangang) and Brown Line (Taipei Nangang Exhibition Center–Taipei Zoo) of TMRT and the Red Line of KMRT (Figure 4). The input data used in the case study were provided by the operators of TMRT and KMRT.

Blue Line in TMRT

The Blue Line is not only a high-capacity line, it is TMRT's busiest line; the operator has already reached 100% capacity during the peak hours. The developed capacity models were applied to the potential choke points in this line: the Taipei Main station and the Zhongxiao Fuxing, Yongning, and Nangang stations. Taipei Main and Zhongxiao Fuxing are the main transfer stations of the system with the highest number of passengers boarding and alighting trains. Yongning and Nangang stations are terminal stations where turnback movements may also cause capacity bottlenecks. Because the line has already reached its capacity during the peak hours, this information can be used to validate the capacity models for systems with speed codes.

Table 3 shows the computational results for the Blue Line. The output shows that Zhongxiao Fuxing and Taipei Main stations are the northbound and southbound bottlenecks, respectively. The actual event log reveals that the minimal headway of the Blue Line during peak hour is about 130 to 135 s, which is very close to the results calculated from the proposed model. The operator reported that large numbers of passengers at Zhongxiao Fuxing and Taipei Main lead to considerable dwell time and eventually increase the signal headway. Currently the operation of the Blue Line is reaching its capacity. The result is consistent with the calculation of the proposed model, demonstrating that the model is verified and validated.

Brown Line in TMRT

The Brown Line is a medium-capacity line with smaller train sets than the high-capacity lines in the TMRT system. This line was upgraded to a moving-block system last year to increase its capacity. Three stations were chosen for this case study: Taipei Nangang Exhibition Center station, Taipei Zoo station, and Zhongxiao Fuxing station. The first two stations are terminal stations with rear scissors crossovers. Zhongxiao Fuxing station (different from the Zhongxiao Fuxing station in the Blue Line) is the main transfer station between the Blue and Brown Lines.

The northbound bottlenecks are Zhongxiao Fuxing and Nangang Exhibition Center stations, and the southbound bottlenecks include all three stations analyzed (Table 4). At Taipei Zoo station, the difference in achievable capacity for northbound and southbound is a result of the time for minor cleaning, which only applies to the southbound traffic.

Red Line in KMRT

KMRT is a fairly new rapid transit system with a distance-to-go signaling system. The Red Line is KMRT's busiest line. Among the six stations selected for this case study, the Kaohsiung, Zuoying, and Formosa stations are the major transfer stations, and the Siaogang, Ciaotou, and Gangshan South stations are the terminal stations. The intermediate station, Ciaotou, is now the temporary terminal station because Gangshan South is still under construction. There is no crossover near Ciaotou station, so trains have to perform the turnback movements by using the forward scissors crossover at Gangshan South as the rear scissors crossover of Ciaotou; the distance of this crossover from Ciaotou (about 2 km) causes considerable operational difficulties.

Table 5 shows the results of this case study for KMRT. As expected, the current bottleneck for both the northbound and southbound traffic is Ciaotou station because of the long turnback time. This bottleneck will shift to Gangshan South station when it is completed, but the opening of the new station will nevertheless improve system line capacity from 16 transit units per hour (TU/h) to 25 TU/h.

CONCLUSION

The assessment of level of service and rail capacity plays an important role in monitoring the performance of an existing system and determining whether to undertake new resource planning projects. A set of comprehensive capacity models was developed with consideration of modern signaling systems, including systems with speed codes, distance to go, and moving blocks, as well as a complete set of possible movements at critical track layouts. Several appropriate values were also recommended for a separation safety factor for various types of signaling system according to the operating data provided by the rail transit operators. The proposed capacity models can help operators easily monitor their systems' performance and identify critical bottlenecks in the systems.

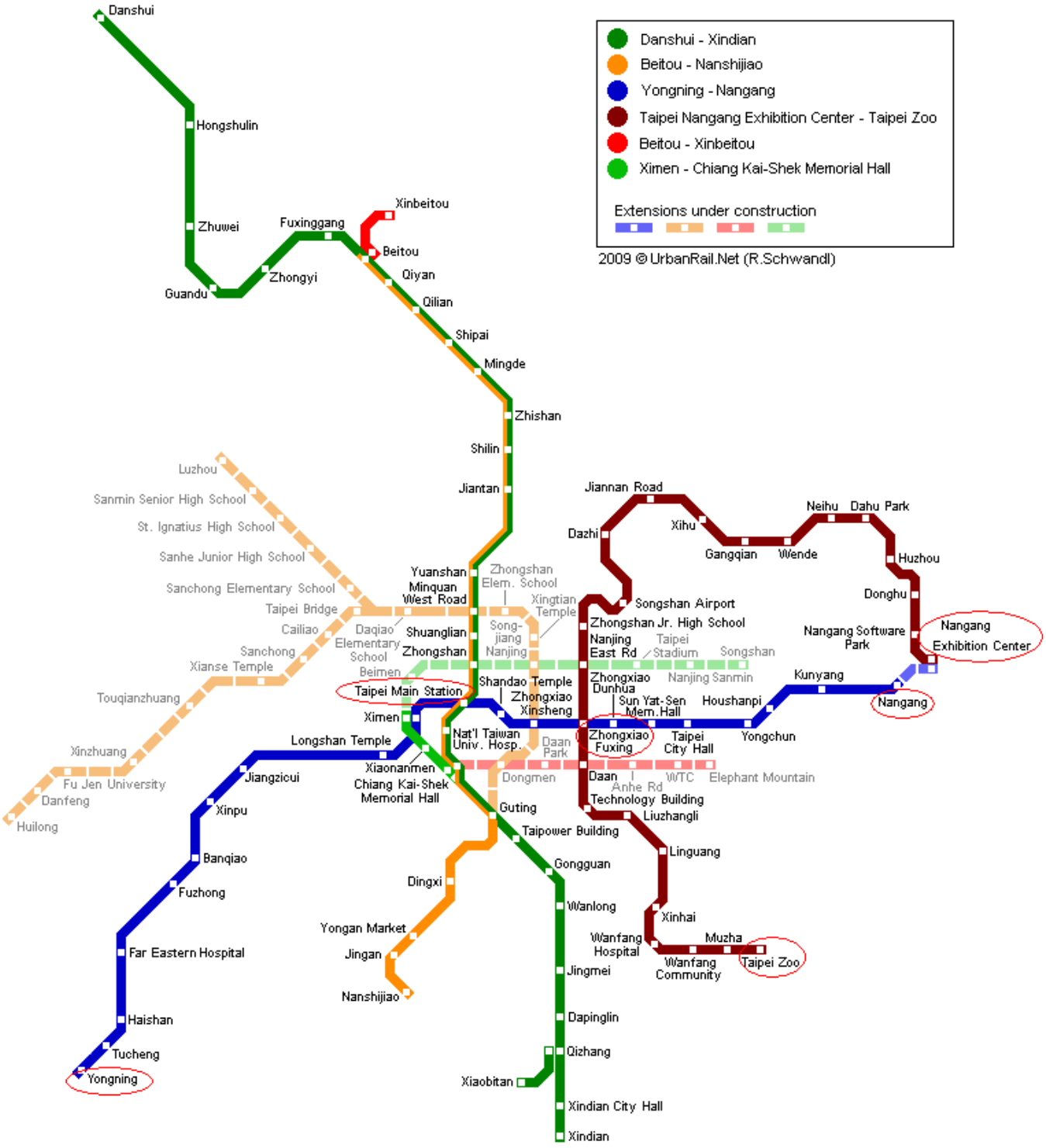

(a)

FIGURE 4 Network maps: (*a*) TMRT system.

(continued on next page)

(b)

FIGURE 4 *(continued)* Network maps: (*b*) KMRT system (*26*).

TABLE 3 Capacity Computation Results of Northbound and Southbound TMRT Blue Line

Station	Type of Track Layout	Average Headway (s)	Line Capacity (TU/h)	Design Capacity (sps/h)	Achievable Capacity (prs/h)
Northbound					
Yongning	III	125	28	54,208	46,076
Taipei main station	I	112	32	61,952	52,659
Zhongxiao Fuxing	I	130	27	52,272	44,431
Nangang	III	124	28	54,208	46,076
Southbound					
Nangang	III	124	28	54,208	46,076
Zhongxiao Fuxing	I	111	32	61,952	52,659
Taipei main station	I	130	27	52,272	44,431
Yongning	III	125	28	54,208	46,076

TABLE 4 Capacity Computation Results of Northbound and Southbound TMRT Brown Line

Station	Type of Track Layout	Average Headway (s)	Line Capacity (TU/h)	Design Capacity (sps/h)	Achievable Capacity (prs/h)
Northbound					
Taipei Zoo	V	55	65	27,976	22,380
Zhongxiao Fuxing	I	90	40	17,216	13,772
Nangang exhibition center	V	90	40	17,216	13,772
Southbound					
Nangang exhibition center	V	90	40	17,216	13,772
Zhongxiao Fuxing	I	90	40	17,216	13,772
Taipei Zoo	V	89	40	17,216	13,772

TABLE 5 Capacity Computation Results of Northbound and Southbound KMRT Red Line

Station	Type of Track Layout	Average Headway (s)	Line Capacity (TU/h)	Design Capacity (sps/h)	Achievable Capacity (prs/h)
Northbound					
Siaogang	III	112	32	24,208	19,366
Formosa Boulevard	I	97	37	27,997	22,392
Kaohsiung Station	I	90	40	30,260	24,208
Zuoying	I	89	40	30,260	24,208
Ciaotou	III	217	16	12,104	9,683
Gangshan South[a]	III	144	25	18,913	15,130
Southbound					
Gangshan South[a]	III	144	25	19,913	15,130
Ciaotou	III	217	16	12,104	9,683
Zuoying	I	100	36	27,234	21,787
Kaohsiung Station	I	86	41	31,016	24,812
Formosa Boulevard	I	102	35	26,477	21,181
Siaogang	III	112	32	24,208	19,366

[a]Under construction.

REFERENCES

1. Kittelson & Associates, Inc., KFH Group, Inc., Parsons Brinckerhoff Quade & Douglass, Inc., and K. Hunter-Zaworski. *TCRP Report 100: Transit Capacity and Quality of Service Manual*, 2nd ed. Transportation Research Board of the National Academies, Washington, D.C., 2003.
2. Edwards, T., and S. Smith. *Transport Problems Facing Large Cities*. Briefing paper No. 6/08. New South Wales Parliamentary Library Research Service, 2008.
3. Litman, T. *Rail Transit in America: Comprehensive Evaluation of Benefits*. Victoria Transport Policy Institute, Victoria, British Columbia, Canada, 2010.
4. Krueger, H. Parametric Modeling in Rail Capacity Planning. *Proc., Winter Simulation Conference*, Phoenix, Ariz., 1999.
5. Abril, M., F. Barber, L. Ingolotti, M. A. Salido, P. Tormos, and A. Lova. An Assessment of Railway Capacity. *Transportation Research Part E*, Vol. 44, No. 5, 2008, pp. 774–806.
6. Matsumoto, M. Breakthroughs in Japanese Railways, 2: Learning from Past Railway Accidents: Progress of Train Control. *Japan Railway and Transport Review*, No. 43–44, 2006, pp. 86–98.
7. Vincze, B., and G. Tarnai. Evolution of Train Control Systems. *Proc., 14th International Symposium Eurnex*, Zilina, Slovak Republic, 2006.
8. Hsiao, Y. T., and K. C. Lin. Measurement and Characterization of Harmonics on Taipei MRT DC System. *IEEE Transaction Industry Application*, Vol. 40, No. 6, 2004, pp. 1700–1704.
9. Jadhav, R. CBTC: Bombardier CITYFLO Solutions. *Proc., IRSE Technical Convention*, Singapore, 2005.
10. Ke, B. R. *Signaling System for Saving Energy on Mass Rapid Transit Systems*. PhD dissertation. National Taiwan University of Science and Technology, Taipei, 2006.
11. Jong, J. C., C. K. Lee, L. S. Lu, E. F. Chang, S. H. Huang, and Y. C. Li. *Capacity Analysis of Rail Transportation System and Its Applications (3/4)*. MOTC-IOT-97-PDB004. Institute of Transportation, Ministry of Transportation and Communication, Taiwan, 2008.
12. Jong, J. C., C. K. Lee, Y. C. Lai, and S. H. Huang. *Capacity Analysis of Rail Transportation System and Its Applications (4/4)*. MOTC-IOT-97-PDB004. Institute of Transportation, Ministry of Transportation and Communication, Taiwan, 2010.
13. Thurston, D. F. Signaling and Capacity Through Computer Modeling. *Proc., International Conference on Computer Modeling for Rail Operations*, Delray Beach, Fla., 2004.
14. Railway Technical Web Pages. ATP Beacons and Moving Block. www.railway-technical.com/. Accessed April 5, 2010.
15. Takashige, T. Signaling Systems for Safe Railway Transport. *Japan Railway and Transport Review*, No. 21, 1999, pp. 44–50.
16. Matsumoto, M. The Revolution of Train Control Systems in Japan. *Proc., Autonomous Decentralized Systems*, Chengdu, China, 2005.
17. Moore Ede, W. J. How CBTC Can Increase Capacity. *Railway Age*, April 2001, pp. 49–50.
18. Li, K. P., Z. Y. Gao, and B. Ning. Cellular Automaton Model for Railway Traffic. *Journal of Computational Physics*, Vol. 209, No. 1, 2005, pp. 179–192.
19. Mattalia, A. *The Effects on Operation and Capacity on Railways Deriving from the Switching to Continuous Signals and Tracing Systems (ERTMS)*. Master's thesis. Department of Transportation and Logistics, Royal Institute of Technology, Stockholm, Sweden, 2007.
20. *Influence of ETCS on Line Capacity: Generic Study*. International Union of Railways, Paris, 2008.
21. Pachl, J. *Railway Operation and Control*. VTD Rail Publishing, Mountlake Terrace, Wash., 2002.
22. Parkinson, T., and I. Fisher. *TCRP Report 13: Rail Transit Capacity*. TRB, National Research Council, Washington, D.C., 1996.
23. Jong, J. C., E. F. Chang, and S. H. Huang. A Railway Capacity Model for Estimating Hourly Throughputs with Mixed Traffic and Complex Track Layouts. *Proc., 3rd International Seminar on Railway Operations Modelling and Analysis*, Zurich, Switzerland, 2009.
24. *UIC Code 406 Capacity*. International Union of Railways, Paris, 2004.
25. Vuchic, V. R. *Urban Public Transportation Systems and Technology*. Prentice Hall, Inc., Englewood Cliffs, N.J., 1981.
26. *Kaohsiung*. www.urbanrail.net/index.html. Accessed April 5, 2010.

The Transit Capacity and Quality of Service Committee peer-reviewed this paper.